Submitted J. Amer. Ceram. Soc.

Elastic Moduli of Pyrolytic Boron Nitride Measured Using 3-Point Bending and Ultrasonic Testing

M. L. Kaforey[a], C. W. Deeb[a], & D. H. Matthiesen[a]

Department of Materials Science & Engineering
Case Western Reserve University
Cleveland, OH 44106

PREPRINT
NAG 8-1268
IN/39

D. J. Roth

NASA Glenn Research Center at Lewis Field
Cleveland, OH 44135

Abstract:

Three-point bending and ultrasonic testing were performed on a flat plate of PBN. In the bending experiment, the deformation mechanism was believed to be shear between the pyrolytic layers, which yielded a shear modulus, c_{44}, of 2.60 ± 0.31 GPa. Calculations based on the longitudinal and shear wave velocity measurements yielded values of 0.341 ± 0.006 for Poisson's ratio, 10.34 ± 0.30 GPa for the elastic modulus (c_{33}), and 3.85 ± 0.02 GPa for the shear modulus (c_{44}). Since free basal dislocations have been reported to affect the value of c_{44} found using ultrasonic methods, the value from the bending experiment was assumed to be the more accurate value.

---

[a] Member of the American Ceramic Society

Based in part on the thesis submitted by C. W. Deeb for the M.S. degree in Materials Science & Engineering, Case Western Reserve University, Cleveland, OH, 1999.

Supported by Microgravity Science & Applications Division, NASA, under grant number NAG8-1268.

1. Introduction

Springs composed of stacks of curved leaves of pyrolytic boron nitride (PBN) have been used in microgravity experiments dealing with solidification processing of semiconductors[1-4]. The springs were used to accommodate the volume change due to the shrinkage of the semiconductor upon melting. In order to design a spring with an appropriate spring constant, the applicable modulus of elasticity for the spring material must be known.

PBN is a highly anisotropic material. The crystal structure is hexagonal with a *c/a* ratio of approximately 2.66 (calculated using lattice parameter values from Pease[5]). Gavrichev[6] reports the spacegroup for this hexagonal structure as $P6_3/mmc$, which results in 5 independent elastic constants[7]. When produced by chemical vapor deposition, the microstructure generally consists of thin, flat plates with the c-axis perpendicular to the substrate surface[8]. For applications such as curved leaf stacks, the elastic modulus needed is that of the pyrolytic microstructure, and not that intrinsic to the hexagonal crystal structure.

Experimental determination of elastic moduli can be done using a variety of techniques. The current work uses both a traditional method, three-point bending, and a nondestructive technique, ultrasonic testing, to determine the elastic moduli of PBN.

Ultrasonic testing measurements have been done by a number of groups[9-11]. This method relates the stiffness of the material to the velocity of the ultrasonic waves in the material and density of the material. Ultrasonic transducers can be designed to produce both longitudinal atomic motion, where the atomic motion is parallel to the direction of propagation of the ultrasonic wave, and shearing/transverse atomic motion, where the atomic motion is

perpendicular to the direction of propagation of the ultrasonic wave. In single crystals, or materials with a high degree of crystallographic texturing, ultrasonic waves can be propagated down particular crystallographic directions to give particular elastic moduli for the material.

2. Experimental Procedure

Three-point bending

A flat plate of PBN (Advanced Ceramics Co., Cleveland, OH) was tested in three-point bending on a mechanical testing system (Instron Model 1125, Instron Corp., Canton, MA). The flat plate measured 37.8 mm (1.49 in.) by 25.6 mm (1.01 in.) by 2.5 mm (0.098 in.). The *c*-direction was parallel to the shortest dimension. The layers in the structure were, therefore, parallel to the broad face. In this microstructural configuration, the layers are perpendicular to the applied load. The support pins had diameters of 6.43 mm (0.253 in.) and 6.35 mm (0.250 in.). The distance between the pins was set to be slightly smaller than the span of the sample. The actual distance between the pins, determined by taking the length from the outside of one pin to the outside of the opposite pin and subtracting the radius of each, was 32.75 mm. The radius of the ram was 4 mm. The crosshead was translated at 0.2 mm/min. The total deflection was preset to 0.1 mm which resulted in an actual deflection of approximately 0.15 mm due to machine limitations.

The data was recorded directly onto chart paper by the mechanical testing system. This was done in lieu of digital recording to obtain continuous data collection. Each cycle consisted of applying a load, pausing until steady state was reached, and unloading the sample. The sample was cycled 7 times and data was recorded for all cycles.

The first two tests were discarded because past experience has shown that irregularities (jaggedness, excessive settling) will generally occur in the first two cycles and then not recur in later cycles. For each of the 5 remaining cycles, the maximum load, P, and the maximum deflection, d, were measured. A value for P/d was calculated for each cycle and the results were averaged. The modulus, E, was then determined using equation (1), which is a rearranged form of the standard equation for bending of a flat plate (see for example Young[12])

$$E = \frac{w^3}{48I}\frac{P}{d} \tag{1}$$

where w is the width of the sample, and I is the moment of inertia given by

$$I = \frac{bh^3}{12} \tag{2}$$

where b is the depth of the sample, and h is the thickness of the sample.

Ultrasonic Testing

The same sample was used for ultrasonic testing as for the three-point bending tests. Ultrasonic testing was done prior to mechanical testing to eliminate concerns about damage occurring in the sample which would affect the ultrasonic measurements. An ultrasonic transducer was placed on the broad surface of the flat plate so that wave propagation would be in the c-axis direction. An ultrasonic signal was passed through the sample. The first transducer used sent a longitudinal signal through the sample. In the longitudinal case, the atomic vibration caused by the wave was parallel to the wave propagation. The speed of this wave in the material was determined from the time between the original signal and the echo from the back surface of

the sample since the thickness of the sample is known. A cross-correlation algorithm[13] was used to precisely determine the time delay between the echoes.

Equation (3) relates the sample density, ρ, Poisson's ratio, ν, and the velocity of the longitudinal ultrasonic wave, V_l, to the elastic modulus, E, according to ref[14]:

$$E = \frac{\rho V_l^2 (1+\nu)(1-2\nu)}{(1-\nu)} \tag{3}$$

The elastic constant in this case corresponded to the principal stress-strain response perpendicular to the face of the sample. For the PBN sample, this would be the elastic constant along the *c*-axis (c_{33}).

A second transducer was used to measure the shear modulus. This transducer sent a signal in which the atomic motion was perpendicular to the wave propagation of the signal. Again, the velocity of the wave through the sample was determined by the time between the original signal and the echo from the back surface of the sample. Equation (4) relates the sample density and the velocity of the ultrasonic shear wave, V_s, to the shear modulus, G, according to ref[14]:

$$G = \rho V_s^2 \tag{4}$$

The elastic constant in this case was therefore the elastic constant relating a shear stress in the a-plane to a shear strain between a-planes ($c_{44} = c_{55} = c_{2323} = c_{1313}$)[7].

Poisson's ratio can also be calculated from the ultrasonic wave velocities using the following equation[14]:

$$\nu = \frac{\left(\frac{V_l^2}{2} - V_s^2\right)}{\left(V_l^2 - V_s^2\right)} \tag{5}$$

Although the derivation for the ultrasonic determination of elastic moduli assumes an isotropic medium, application to this case can be justified. Due to the high degree of *c*-axis texturing, the ultrasonic waves are propagated approximately along the *c*-axis, and the material is isotropic within the basal plane. Thus, the material is isotropic about the axis of propagation, allowing the use of this method.

3. Results

A typical chart recording for one cycle of the flat plate is shown in Fig. 1. The loading curve increased monotonically. There was a very small loading transient, most likely due to settling of the contact points. The bulk of the loading curve was linear to the maximum load. There was a small inflection in the unloading curve that was believed to be due to the machine behavior and not due to the behavior of the material. The data from the cycles are given in Table 1. The average *P/d* value was 127.7 ± 15.3 N/mm. Using equation (1), this yields a modulus of 2.60 ± 0.31 GPa.

To determine the contribution of the apparatus on the data, experiments using flat plates of fused quartz were performed in the same manner as the flat plate of PBN. A typical chart record from a three-point bend test performed using a flat plate of quartz is shown in Fig. 2.

Quartz was used because its elastic modulus of 71.7 GPa (10.4×10^6 psi) is well established[15]. The load versus deflection data from these experiments was used with equation (1) to calculate the elastic constant obtained via the apparatus used in this work. The calculated modulus of 71.04 ± 3.01 GPa agreed with the reported value of 71.7 GPa within experimental error. The deflection of the apparatus was therefore assumed to be negligible throughout this

work. All curves had loading transients. This was probably due to a combination of settling of the contact points between the sample and the pins, the platen and the load cell, and the ram and the crosshead. All curves also had inflections in the unloading curves. This supports the hypothesis that this is due to the behavior of the machine, not due to the behavior of the material. Both of these loading and unloading effects are assumed to be due to the apparatus since a perfectly isotropic material, such as fused quartz, would not behave differently on loading and unloading.

The values measured from the ultrasonic experiments are given in Table 2. The density of the sample was measured (2.146 ± 0.003 g/cm^3) prior to ultrasonic testing. Each ultrasonic wave velocity measurement was repeated three times with no measurable variation seen between the three experiments. The error stated for the ultrasonic wave velocities are the errors in the cross correlation velocities. The values for Poisson's ratio, the elastic modulus, and the shear modulus are calculated using equations (3) to (5). The value calculated for Poisson's ratio was 0.341 ± 0.006. Ultrasonic testing yielded an elastic modulus, c_{33}, of 10.34 ± 0.30 GPa, and a shear modulus, c_{44}, of 3.85 ± 0.02 GPa.

4. Discussion

The values reported in the literature for the elastic moduli of PBN are given in Table 3. The choice of which elastic constant to use for a given application is non-trivial. These values were determined from a variety of methods including calculations based on thermal conductivity measurements[8], ultrasonic measurements on materials of different interlayer spacing[16], thermal expansion data[17], torsional creep experiments[18], and compression measurements[19-20].

In three-point bending of the flat plate, the failure mechanism would be expected to be delamination of the layers. The combination of stress due to the chemical vapor deposition process and the planar structure of PBN leads to failure by delamination[20]. Thus, the deformation mechanism is shear between the layers, and the modulus measured from the three-point bending experiment should be c_{44}. This value closely matches the value for c_{44} reported by Duclaux[8] for a material of comparable density and structure. Archer[20] notes that elastic bending by basal planes sliding over each other (ε_{44}) contributes to the flexibility of PBN. This also supports the idea that the deformation mechanism is shear between layers.

The value of Poisson's ratio calculated from the ultrasonic measurements using equation (5) was 0.341 while the values reported in the literature are 0.25 (from Advanced Ceramics[19]) and –0.025 (from Basche[21] from hydrostatic pressure tests). The values reported in the literature are for the *a*-direction, while the value calculated here is for the *c*-direction. For an anisotropic material such as PBN, this difference is reasonable.

The value for the elastic modulus from ultrasonic testing is considerably less than the reported values for c_{33} in Table 3. Duclaux[8] determined the relationship between c_{33} and the interlayer distance, δ, to be

$$c_{33} = 18.7 - 672.8(\delta - 0.333)$$

where c_{33} is in GPa and δ is in nm. For the value of c_{33} calculated from the ultrasonic wave velocity of 10.34 GPa, the corresponding interlayer distance is 0.345 nm which, in turn, corresponds to a *c*-lattice parameter of 0.690 nm (6.90 Å). This is a reasonable *c*-lattice parameter for PBN that is only 95 % dense. The good agreement between the current results and

the results of Duclaux lead us to conclude that the current measurement was correct and the theoretical calculation of Kelly[17] based on thermal expansion data was too large.

Density variations can affect the measured wave velocity[22]. Porosity in this plate-like microstructure will tend to reside between plates. This will have an effect on the measured elastic modulus along the *c*-axis, as the porosity directly impedes the transmission of atomic motion perpendicular to the plates. This porosity will result in a reduction in the calculated value for c_{33}. That is, the value of c_{33} calculated from equation (3) for a fully dense material should be slightly higher than the value calculated from these tests since both the ultrasonic wave velocity and the density would be larger. However, PBN made by chemical vapor deposition is typically 96 % dense so the c_{33} value of 10.34 GPa should apply to most PBN.

The value for the shear modulus from the ultrasonic tests is larger than the highest reported value for c_{44} and the value from the three point bending tests. Duclaux[8] reports that the value of c_{44} is a function of microstructure, but the relation for c_{44} is not as straightforward as for c_{33}. Duclaux[8] reported values of c_{44} for BN samples ranging from <0.01 GPa for a turbostratic sample to 1.54 GPa and 2.52 GPa for other samples. They attributed the decrease in c_{44} in some samples to the presence of free basal dislocations and point defects such as vacancies or interstitial atoms. They noted that ultrasonic methods used to determine c_{44} in PBN were affected by the presence of free basal dislocations. Thus, the value for c_{44} found using three-point bending was taken to be the more accurate value for c_{44}.

5. Conclusions

A flat plate of PBN tested in three point bending yielded an effective elastic modulus of 2.60 ± 0.31 GPa. Since the mechanism of deformation is believed to be shear between layers in the pyrolytic structure, this value was assigned to the shear modulus, c_{44}. This value closely matched the values reported for c_{44} in the literature.

Ultrasonic measurements were performed on a flat plate of PBN to determine the elastic modulus and the shear modulus. The ultrasonic wave velocity measurements performed on the same flat plate of PBN yielded values for Poisson's ratio of 0.341 ± 0.006, for the elastic modulus, c_{33}, of 10.34 ± 0.30 GPa and for the shear modulus, c_{44}, of 3.85 ± 0.02 GPa. Since free basal dislocation have been reported to affect c_{44} values determined using ultrasonic methods, the value of c_{44} found in three-point bend testing (2.60 GPa) was assumed to be the more accurate value.

6. References

1. M. L. Kaforey, J. M. Bly and D. H. Matthiesen, "Void Formation in Gallium Arsenide Crystals Grown in Microgravity." J. Cryst. Growth **174**, 112-119 (1997).
2. D.H. Matthiesen and J.A. Majewski, "The Study of Dopant Segregation Behavior During the Growth of GaAs In Microgravity"; pp. 232-262 in NASA Joint Launch 1 Year Science Review, Vol. 1. NASA Conference Publication 3272, May 1994.
3. D.H. Matthiesen, M.L. Kaforey, and J.M. Bly, "Experiment XIII. The Study of Dopant Segregation Behavior During the Growth of GaAs in Microgravity on USML-2"; pp. 293-

335 in Second United States Microgravity Laboratory: One Year Report, Vol. 1. NASA TM-1998-208697, August 1998.

4. J.M. Bly, M.L. Kaforey, D.H. Matthiesen, and A. Chait, "Interface Shape and Growth Rate Analysis of Se/GaAs Bulk Crystals Grown in the NASA Crystal Growth Furnace (CGF)," J. Cryst. Growth **174**, 220-225 (1997).
5. R.S. Pease, "An X-ray Study of Boron Nitride," Acta Cryst. **5**, 356-361 (1952).
6. K.S. Gavrichev, V.L. Solozhenko, V.E. Gorbunov, L.N. Golushina, G.A. Totrova, and V.B. Lazarev, "Low-temperature Heat Capacity and Thermodynamic Properties of Four Boron Nitride Modifications," Thermochimica Acta **217**, 77-89 (1993).
7. J.F. Nye: *Physical Properties of Crystals: Their Representation by Tensors and Matrices.* (Oxford University Press, New York, 1985).
8. L. Duclaux, B. Nysten, J-P. Issi, and A.W. Moore, "Structure and Low-temperature Thermal Conductivity of Pyrolytic Boron Nitride," Phys. Rev. B **46** [6] 3362-3367 (August 1992).
9. D.J. Roth, M.R. DeGuire, and L.E. Dolhert, "Ultrasonic Evaluation of Oxygen Content, Modulus, and Microstructure Changes in $YBa_2Cu_3O_{7-x}$ Occurring During Oxidation and Reduction," J. Am. Ceram. Soc. **75** [5] 1182-90 (1992).
10. H. Ledbetter, S. Kim, and D. Balzar, "Elastic Properties of Mullite," J. Am. Ceram. Soc. **81** [4] 1025-1028 (1998).
11. Y.C. Chu and S.I. Rokhlin, "Determination of Macromechanical and Micromechanical and Interfacial Elastic Properties of Composites from Ultrasonic Data," J. Acoust. Soc. Am. **92** [2] 920-931 Part 1 (August 1992).

12. W.C. Young, *Roark's formulas for stress and strain*, 6th ed. (McGraw-Hill, New York, 1989).

13. D.R. Hull, H.E. Kautz, and A. Vary, "Measurement of Ultrasonic Velocity Using Phase-Slope and Cross-Correlation Methods," Mater. Eval. **43** [11] 1455-1460 (1985).

14. J. Krautkrämer and H. Krautkrämer, *Ultrasonic Testing of Materials*, 4th ed., p. 13-14 (Springer-Verlag, New York, 1990).

15. D.R. Lide, ed., *CRC Handbook of Chemistry and Physics*, 71st ed., p. 12-125 (CRC Press, Boston, 1990) based on information contained in Fused Quartz Catalogue Q-7A General Electric Company.

16. B. Jager, Ph.D. Thesis, Université de Grenoble (1977) as cited in L. Duclaux, B. Nysten, J-P. Issi, and A.W. Moore, "Structure and Low-temperature Thermal Conductivity of Pyrolytic Boron Nitride," Phys. Rev. B **46** [6] 3362-3367 (August 1992).

17. B.T. Kelly, "The Anisotropic thermal expansion of boron nitride II. Interpretation by the semi-continuum model," Phil. Mag. **32**, 859-867 (1975).

18. G. Pezzotti, H-J. Kleebe, K. Ota, and T. Nishida, "Internal friction and torsional creep behavior of chemically vapor deposited boron nitride," J. Mater. Res. **13**, 3453-3457 (1998).

19. Union Carbide Corporation (Advanced Ceramics Corporation), "Boralloy: Pyrolytic Boron Nitride." Corporate literature (1987).

20. N.J. Archer, "The Preparation and Properties of Pyrolytic Boron Nitride" pp. 167-180 in "High Temperature Chemistry of Inorganic Ceramic Materials: Proceedings of a Conference," Chemical Society Special Publication Number 30 (1977).

21. M. Basche and D. Schiff, "New Pyrolytic Boron Nitride," Materials in Design Engineering 78-81 (February 1964).

22. D.J. Roth, D.B. Stang, S.M. Swickard, M.R. DeGuire, and L. E. Dolhert, "Review, Modeling and Statistical Analysis of Ultrasonic Velocity-Pore Fraction relations in Polycrystalline Materials," Mater. Eval. **49** [7] 883-888 (1991).

7. Figure Captions

Figure 1. Load versus deflection chart recording from cycle 7 for the flat plate PBN experiment with maximum load, P = 4.52 lbf = 20.1 N and maximum deflection, d = 0.17 mm (0.500 lbf=2.224 N).

Figure 2. Load versus deflection chart recording for one cycle of the flat plate fused quartz experiment with maximum load, P = 3.15 lbf = 14.0 N and maximum deflection, d = 0.64 mm (0.500 lbf=2.224 N).

Table 1. Results of three-point bend tests.

Cycle	Maximum load, P (N)	Maximum deflection, d (mm)	P/d (N/mm)	Resultant Modulus, E (GPa)
3	16.2	0.14	115.4	2.35
4	15.7	0.12	131.0	2.67
5	18.0	0.15	120.2	2.45
6	20.6	0.13	153.0	3.12
7	20.1	0.17	119.1	2.43
Average of cycles 3-7:			127.7 +/- 15.3	2.60 +/- 0.31

Table 2. Results of ultrasonic testing.

Property	Determined Value
Density (measured prior to ultrasonic testing), ρ (g/cm^3)	2.146 ± 0.003
Measured Longitudinal Velocity, V_l (cm/μsec)	0.273 ± 0.0005
Measured Shear Velocity, V_s (cm/μsec)	0.134 ± 0.0003
Calculated Poisson's Ratio, ν	0.341 ± 0.006
Calculated Elastic Modulus, E (GPa)	10.35 ± 0.30
Calculated Shear Modulus, G (GPa)	3.85 ± 0.02

Table 3. Reported Values for the Elastic Moduli of PBN.

C_{11}	C_{33}	C_{12}	C_{13}	C_{44}	$E_{//a}$	$E_{//c}$	Ref.
				2.52 1.54			Duclaux[8]
750	18.7	150					Jager[14]
830	29.5	13	50	0			Kelly[15]
			7.8				Pezzotti[16]
					22	4.76	Advanced Ceramics[17]
					19.6	6.9	Archer[18]
				2.60			Current work - 3 point bending
	10.34			3.85			Current work – ultrasonic testing

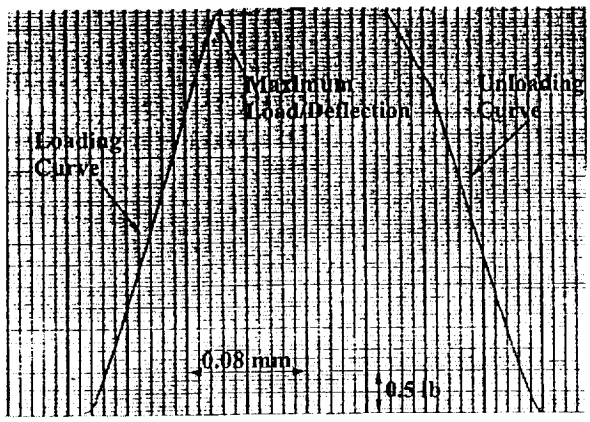

Figure 1. Load versus deflection chart recording from cycle 7 for the flat plate PBN experiment with maximum load, P = 4.52 lbf = 20.1 N and maximum deflection, d = 0.17 mm (0.500 lbf=2.224 N).

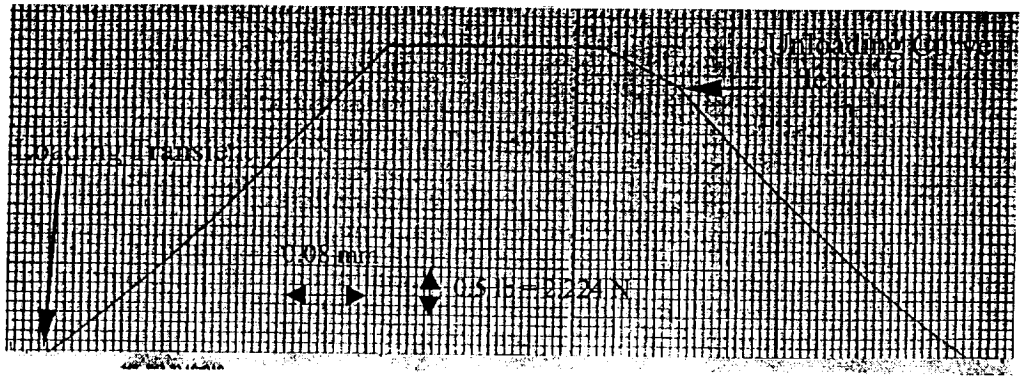

Figure 2. Load versus deflection chart recording for one cycle of the flat plate fused quartz experiment with maximum load, $P = 3.15$ lbf = 14.0 N and maximum deflection, $d = 0.64$ mm (0.500 lbf=2.224 N).